Available online at www.sciencedirect.com

SciVerse ScienceDirect

Physics Procedia 45 (2013) 233 – 236

Physics Procedia

ISS2012

Development of a flat-plate cryogenic oscillating heat pipe for improving HTS magnet cooling

K. Natsume*, T. Mito, N. Yanagi, H. Tamura

National Institute for Fusion Science, 322-6 Oroshi-cho Toki, Gifu 509-5292, Japan

Abstract

A new method of including cryogenic oscillating heat pipes (OHPs) in the HTS coil windings as a thermal transport device has been studied. In this work, two type of OHPs are tested in low temperature. Employed working fluids are H_2, Ne, N_2. We have attained high performance thermal property using a bent-pipe cryogenic OHP as a prototype. Obtained effective conductivities have reached to 46000 W/m·K. Then a flat-plate cryogenic OHP has been developed, that is suitable for imbedding in magnet windings. Preliminary experiments have been conducted and the result has been promising.

Selection and/or peer-review under responsibilty of ISS Program Committee.

Keywords: Oscillating heat pipe; Pulsating heat pipe; Superconducting magnet; HTS; Heat transport

1. Introduction

A new methodology which thin cryogenic oscillating heat pipes (OHPs) are embedded into inter-space of coil windings as heat transfer devices has been suggested in order to improve the efficiency of conduction cooling of HTS magnets [1]. OHPs were proposed and patented by Akachi [2]. Those are highly effective heat transfer devices which can transport several orders of magnitude greater heat flux than the heat conduction of solids and be formed in a thin plate structure. In these respects, we consider that the OHPs embedded in the coil windings can enhance the heat removal characteristics in HTS magnets.

Fig. 1 shows the concept of the heat transfer mechanism of OHP. OHP generally consists of a capillary tube wound in serpentine manner and jointed the ends to the inlet. A two-phase mixture distributes in the form of liquid slugs and vapour bubbles inside the capillary tube. When the one end of the tube is heated (the evaporator), the working fluid causes bubbles to grow and increases the vapour pressure. At the same time, bubbles condense and the vapour pressure decreases in another end (the condenser) that is kept the temperature low enough to liquefy the working gas. The growth and collapse of bubbles in the evaporator and the condenser sections, respectively, results in an oscillating motion with in the tube. The heat is transferred through latent heat in vapours and sensible heat by liquid slugs[3]. As a result of our previous studies, the cryogenic OHP has achieved the stable operation in a wide temperature range with the high effective thermal conductivity and the quick response time [1,4-7].

Fig. 2 illustrates a conceptual design configuration of a HTS magnet with the OHP cooling. The cooling panels that include OHPs are inserted between each double pancake coil windings.

2. Experimental set-up

Fig. 3 shows the experimental set-up for cryogenic operation tests. A foil heater is attached to the surface of the bottom part of the OHP to make a evaporator. On the other hand, the upper part is connected to the cold head

*Corresponding author. Tel.:+81-572-58-2222; fax: +81-572-58-2616.
E-mail address: natsume@nifs.ac.jp.

1875-3892
Selection and/or peer-review under responsibilty of ISS Program Committee.
doi:10.1016/j.phpro.2013.05.010

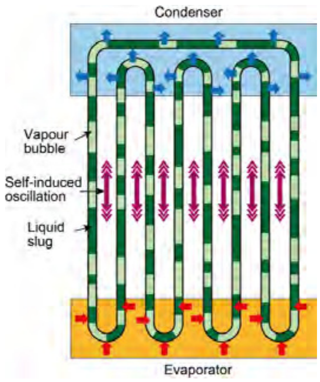

Fig. 1. Schematic representation of oscillating heat pipe

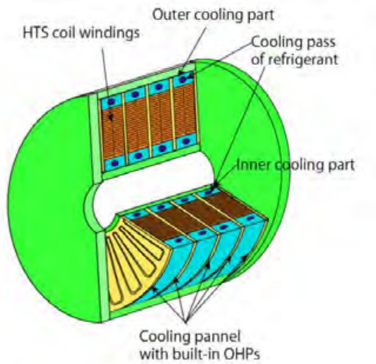

Fig. 2. Conceptual design of the OHP cooling HTS magnet

of the GM cryocooler with copper bus-bar to make a condenser. Resistive thermometers are attached on the OHP at the surfaces of the evaporator and the condenser in order to investigate heat transport characteristics of the OHP. The testing OHP is covered with the radiation shield and installed in the vacuum vessel. The inlet of the working fluid is connected to the buffer tank through an isolation valve. The pressure gauges are installed in the buffer tank and the filling pipe, which are used to control the amount of working fluid to the OHP and to monitor the self-oscillation of the OHP. The working fluid can be changeable among H_2, Ne and N_2 according to the operation temperature.

The heat transport characteristics of the OHP has been investigated by observing the temperature of the evaporator and condenser by changing the heater power, the liquid filling ratio of the working fluid, and the kind of working fluid. The effective thermal conductivity *k* is defined as :

$$k = \frac{\dot{Q}}{\Delta T} \times \frac{L}{S}$$

Where $\dot{Q}, \Delta T, L, S$ represents heat input to the evaporator, temperature difference between the evaporator and condenser, distance from the center of the evaporator to the center of the condenser and the summation of cross sectional area of fluid channels for bent-pipe OHPs or the cross sectional area of the whole plate for flat-plate cryogenic OHPs.

3. Results

3.1. Bent-pipe OHP

Fig. 4 shows the photograph of a bent-pipe OHP. It comprises an evaporator section and a condenser section made of copper block and a capillary made of stainless steel bent into 10 turns between the sections. The outer and inner diameter of the capillary tube is 2 mm and 1 mm respectively. The Cu block of 13 mm in thickness and 30 mm in length has rectangular holes according to the pipe positions. The Cu block and the capillary are soldered in these holes. The distance between two sections is 230 mm, that means L is 260 mm.

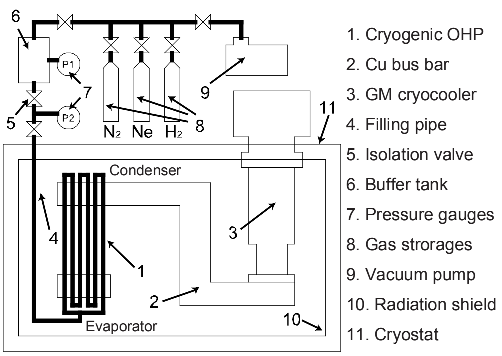

Fig. 3. Experimental set-up for cryogenic operation tests

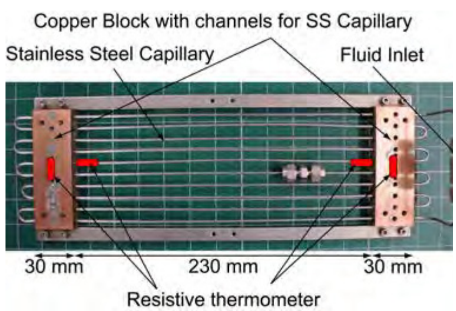

Fig. 4. Photograph of a bent-pipe OHP

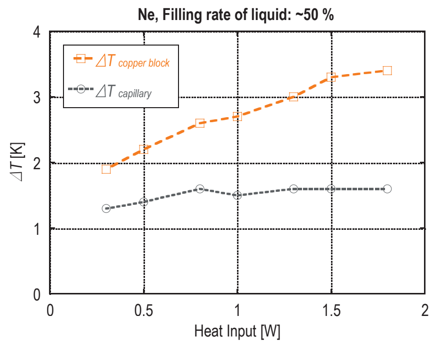

Fig. 5. Comparison of temperature diffrences on the OHP.

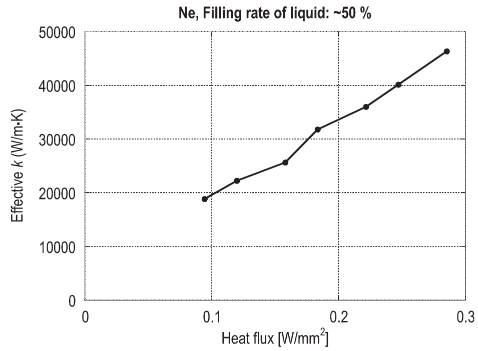

Fig. 6. Thermal conductivity of a bent pipe OHP.

Fig. 5 shows the comparison of measured ΔT for thermometers on Cu blocks and the capillary. The condenser temperature is kept to maintain at about 27 K in this operation. It has been found that the temperature gradient in Cu blocks is dominant in the temperature difference between the evaporator and condenser. Effective thermal conductivities estimated from the data of thermometers attached on capillary directly are shown in Fig. 6. The heat flux is caluculated by the heat input into the condenser and the crosssectional area of the OHP. Obtained effective conductivities have reached to 46000 W/m·K. For comparison, the thermal conductivity of Cu with a residual resistivity ratios of 100 is about 2000 W/m·K at 20 K. It has been confirmed that the thermal transportation property of the OHP is much higher than that of solid conductions. However, bent-pipe OHPs are not suitable for real applications because inter-spaces between bent capillaries cannot contribute to any thermal or mechanical performance.

3.2. Flat-plate OHP

The basic design concept of a flat-plate cryogenic OHP is shown in Fig. 7. The structure of a flat-plate cryogenic OHP refers to that of the 3D FP-OHP described in [8]. The 3D FP-OHP is a flat plate OHP with three-dimensional channel, where two layers of square channels are utilized to increase the channel density. A number of grooves are milled on each side of the base plate. Connecting grooves and holes are made at the end of each channel – allowing for the three-dimensional, inter-twining flow channel configuration. Then the base plate is braze-sealed with two thin cover plates. Fig. 8. is the photograph of a manufactured flat-plate OHP for cryogenic experiments. External size is 5 mm in thickness, 95 mm in width, and 225 mm in length. One channel has a square section of 1.5 mm × 1.5 mm, and the length of the channel is 200 mm. Total of 22 channels are composed and the cross-sectional area (1.5 × 1.5 × 22 = 49.5 mm^2) of the 22 channels filled with the working fluid is 10.4 % against total cross section (95 × 5 = 475 mm^2) of the flat-plate cryogenic OHP.

Fig. 9 shows a typical pressure oscillation of the flat-plate OHP for H_2. The frequency and the amplitude of the oscillation depend on experimental conditions: kind of working fluid, heat input, filling rate of liquid and so forth. It is confirmed that the manufactured OHP operates stably.

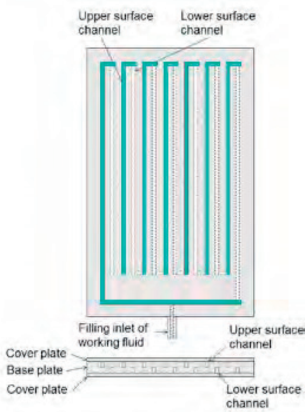

Fig. 7. Basic design of the flat-plate OHP

Fig. 8. Picture of the flat-plate OHP

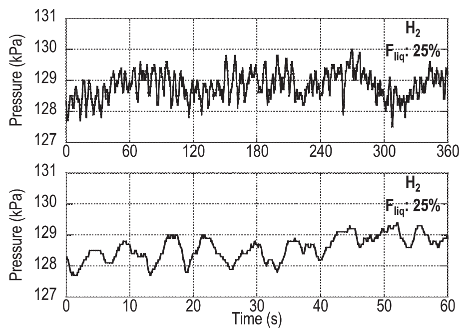

Fig. 9. Pressure oscillation of a flat-plate OHP

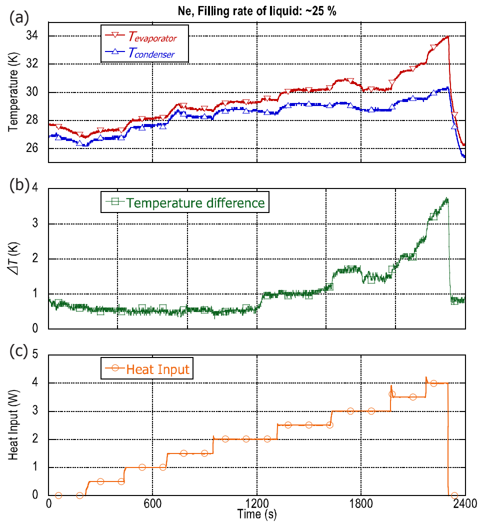

Fig. 10. Temperature data of a flat-plate OHP experiment with heat input using Ne as the working fluid of ~25 % in the liquid filling rate.

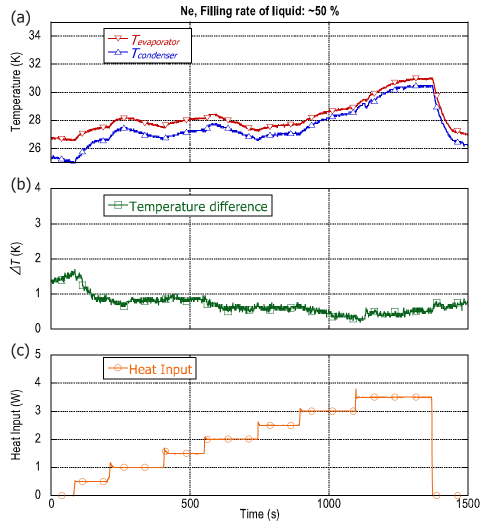

Fig. 11. Temperature data of a flat-plate OHP experiment with heat input using Ne as the working fluid of ~50 % in the liquid filling rate.

Fig. 10 and Fig. 11 present experimental data of the flat-plate OHP using Ne as the working fluid of ~25 % and ~50 % in the filling rate of liquid. Fig. 10(a) and 11(a) show the temperatures at the condenser part and the evaporator part of the OHP. Both temperatures changed depending on the heat input of the heater (Fig. 10(c) and 11(c)). The temperature difference between the evaporator and condenser is plotted in Fig. 10(b) and 11(b). It was shown that the temperature difference is kept about 1.5 K. When heat input is above 3 W, however, the temperature difference of the OHP of ~25 % in the liquid filling rate has been increased. It has been considered that in this experimental condition a lack of fluid inside the OHP take places reducing the thermal transport property.

4. Summary

Table 1 shows the summarized result of experiments for flat-plate OHPs. The effective thermal conductivities have been increased with the heat input generally, except in the lack of liquid condition. It has been thought that the self-induced fluid vibration is activated in proportion to the heat input. The effective thermal conductivities have been reached 850 W/m·K for H_2, 2,500 W/m·K for Ne and 3,500 W/m·K for N_2. Considering the sectional area of the channels is 10.4 % of the total cross section of the OHP, these values must be consistent with the result of bent-pipe OHP experiments. These primary experiments of the flat-plate OHP has been successfully conducted. The thermal transport property will be improved by further optimizations of the design of the OHP.

Table 1. Characteristics of the flat-plate OHP

Working fluid	Operating temperature (K)	Filling rate of Liquid (%)	Effective thermal conductivity (W/m·K)
H_2	18-24	23-60	~850
Ne	26-32	23-53	~2500
N_2	79-84	22-43	~3500

References

[1] T. Mito, K. Natsume, N. Yanagi. H. Tamura, T. Tamada, K. Shikimachi et al., IEEE Trans. Appl. Supercond. 20 (2010) 2023-2026.
[2] H. Akachi, US Patent No. 4,921041, 1990.
[3] D.A. Reay, P.A. Kew, Heat Pipes -theory, design and applications-, fifth ed., Butterworth-Heinemann, 2006.
[4] T. Mito, K. Natsume, N. Yanagi. H. Tamura, T. Tamada, K. Shikimachi et al., IEEE Trans. Appl. Supercond. 21 (2011) 2470-2473.
[5] K. Natsume, T. Mito, N. Yanagi. H. Tamura, T. Tamada, K. Shikimachi et al., Cryogenics 51 (2011) 309-314.
[6] K. Natsume, T. Mito, N. Yanagi. H. Tamura, T. Tamada, K. Shikimachi et al., Proceedings of ICEC23-ICMC 2010 (2011) 991-995.
[7] K. Natsume, T. Mito, N. Yanagi. H. Tamura, T. Tamada, K. Shikimachi et al., IEEE Trans. Appl. Supercond. 22 (2012) No. 4703904.
[8] S.M. Thompson, P. Chneg, H.B. Ma, International Journal of Heat and Mass Transfer 54 (2011) 3951-3959.